Journal of Applied Mechanics and Technical Physics, Vol. 46, No. 5, pp. 624–634, 2005

THERMOMECHANICAL BEHAVIOR OF ELECTRICALLY CONDUCTING SOLIDS EXPOSED TO AN EXTERNAL ELECTROMAGNETIC FIELD

B. D. Drobenko

UDC 539.3: 538.3: 536.21: 518.12

This paper describes a procedure for the mathematical and numerical modeling of the thermomechanical behavior of electrically conducting solid bodies exposed to an external electromagnetic field. The constitutive equations for the electromagnetic field are the Maxwell equations written for the region of the solid body and the ambient medium. The stress–strain state of the solid is described using the relations for nonisothermal elastoplastic flow. The effects of the electromagnetic field on the heat-transfer and deformation processes are taken into account via heat release and ponderomotive forces, respectively. The relations between the electric and magnetic inductions and the corresponding field strengths are considered nonlinear. All physicomechanical parameters of the body material are temperature dependent.

Key words: *thermomechanics of electrically conducting solids, coupled fields, high-temperature induction heating.*

Introduction. Electromagnetic fields (EMFs) are widely used in modern solid-processing technologies, in particular, for induction heating intended to increase the strength and reliability. Existing computational models of such heating examine predominantly coupled electromagnetic and thermal processes [1–5] or in some cases, together with mechanical processes [6, 7], using a number of simplifications for the interaction of the processes (nonferromagnetic materials, temperature-independent characteristics, and elastic deformation). In the cases where the solids are heated to high temperatures, such models can lead to both quantitative and qualitative considerable errors. Thus, for example, steels undergo predominantly plastic deformation even at temperatures of about 550–600°C because of the temperature dependence of the elastic limit [8]. In the heating range of 20 to 1000°C the electric conductivity of steel can vary by a factor of 6 to 8. At the Curie temperature, ferromagnetic materials generally lose ferromagnetic properties and their heating is considerably slowed down. Therefore, there is a practical need for the development of mathematical models that would provide a more realistic description of the interaction of the examined fields of various natures in a solid body exposed to an external EMF in a wide range of temperatures taking into account the nonlinearity of the electromagnetic, thermal, and mechanical properties of the body material.

The present paper describes a procedure for the mathematical and numerical modeling of the thermomechanical behavior of electrically conducting temperature-sensitive solids exposed to an external EMF taking into account the elastoplastic nature of the deformation and the nonlinear dependence between the electric and magnetic inductions and strengths.

1. Formulation of the Problem. We consider an electrically conducting axisymmetric body V in which there are no extraneous electric charges and currents. The body is exposed to an EMF generated by a system of currents located outside the body $\boldsymbol{j}^{(0)}(r,z,t) = (0, j_\varphi^{(0)}(r,z,t), 0)$ (r, φ, and z are cylindrical coordinates). The problem is to determine the electromagnetic and temperature fields due to this effect and the mechanical stresses in the body. The electromechanical, thermoelectric, and magnetostriction effects are considered insignificant and

Podstrigach Institute of Applied Problems of Mechanics and Mathematics, National Academy of Sciences of Ukraine, L'viv 79053; budz@iappm.lviv.ua. Translated from Prikladnaya Mekhanika i Tekhnicheskaya Fizika, Vol. 46, No. 5, pp. 14–26, September–October, 2005. Original article submitted November 22, 2004.

the electric and magnetic inductions and strengths are considered parallel.

For the equations of state

$$\boldsymbol{B}^{(1)} = \boldsymbol{B}_*(\boldsymbol{H}^{(1)}, T), \qquad \boldsymbol{D}^{(1)} = \boldsymbol{D}_*(\boldsymbol{E}^{(1)}, T),$$
$$\boldsymbol{j}^{(1)} = \gamma \boldsymbol{E}^{(1)}, \qquad \boldsymbol{B}^{(0)} = \mu_0 \boldsymbol{H}^{(1)}, \qquad \boldsymbol{D}^{(0)} = \varepsilon_0 \boldsymbol{E}^{(0)}, \tag{1.1}$$

the electromagnetic and temperature fields are described by the following equations [6]:

$$\operatorname{rot} \boldsymbol{H}^{(m)} = \frac{\partial \boldsymbol{D}^{(m)}}{\partial t} + \boldsymbol{j}^{(m)}, \qquad \operatorname{rot} \boldsymbol{E}^{(m)} = -\frac{\partial \boldsymbol{B}^{(m)}}{\partial t}; \tag{1.2}$$

$$c \frac{\partial T}{\partial t} = \nabla \cdot (\lambda \nabla T) + \boldsymbol{j}^{(1)} \boldsymbol{E}^{(1)}. \tag{1.3}$$

Here $\boldsymbol{H} = (H_r(r,z,t), 0, H_z(r,z,t))$ and $\boldsymbol{E} = (0, E_\varphi(r,z,t), 0)$ are the magnetic- and electric-strength vectors, $\boldsymbol{B} = (B_r(r,z,t), 0, B_z(r,z,t))$ and $\boldsymbol{D} = (0, D_\varphi(r,z,t), 0)$ are the magnetic and electric inductions, the quantities with the superscript $m = 0$ refer to the ambient medium (whose electromagnetic properties are described in a vacuum approximation), and those with the superscript $m = 1$ refer to the region of the body, $\boldsymbol{B}_*(\boldsymbol{H}^{(1)}, T)$ and $\boldsymbol{D}_*(\boldsymbol{E}^{(1)}, T)$ are functions that specify the relations between the induction and strength vectors of the magnetic and electric fields, respectively in the body, $\boldsymbol{j}$ is the current density, $\gamma = \gamma(T)$ is the electric conductivity of the body, ε_0 and μ_0 are the dielectric and magnetic permeabilities of vacuum, ∇ is the Hamiltonian, $c = c(T)$ is the volume specific heat, and $\lambda = \lambda(T)$ is the thermal conductivity.

The Maxwell equations (1.2) can be reduced to a system of equivalent relations for one of the functions — $\boldsymbol{E}$ or $\boldsymbol{H}$. Let us write these equations for $\boldsymbol{E}$. With allowance for (1.1), Eqs. (1.2) for the body become

$$\operatorname{rot} \boldsymbol{H}^{(1)} = \varepsilon \frac{\partial \boldsymbol{E}^{(1)}}{\partial t} + \frac{\partial \boldsymbol{D}_*}{\partial T} \frac{\partial T}{\partial t} + \gamma \boldsymbol{E}^{(1)}, \quad \operatorname{rot} \boldsymbol{E}^{(1)} = -[\mu_*] \frac{\partial \boldsymbol{H}^{(1)}}{\partial t} - \frac{\partial \boldsymbol{B}_*}{\partial T} \frac{\partial T}{\partial t}. \tag{1.4}$$

Here

$$[\mu_*] = \begin{bmatrix} \mu_r & 0 \\ 0 & \mu_z \end{bmatrix}; \qquad \mu_r = \frac{\partial B_{*r}}{\partial H_r^{(1)}}, \qquad \mu_z = \frac{\partial B_{*z}}{\partial H_z^{(1)}}; \qquad \varepsilon = \frac{\partial D_{*\varphi}}{\partial E_\varphi^{(1)}}.$$

We multiply the second equation (1.4) by $[\mu_*]^{-1}$, performing the operation rot on both of its sides, and substitute the first equation of (1.4) into the relation obtained. Then, for the single nonzero component of the electric strength vector $\boldsymbol{E}^{(1)}$ in the body, we obtain the equation

$$-\frac{\partial}{\partial r}\Big(\frac{1}{\mu_z}\frac{1}{r}\frac{\partial}{\partial r}(rE_\varphi^{(1)})\Big) - \frac{\partial}{\partial z}\Big(\frac{1}{\mu_r}\frac{\partial E_\varphi^{(1)}}{\partial z}\Big) + \frac{\partial \gamma}{\partial t} E_\varphi^{(1)} + F_q \frac{\partial E_\varphi^{(1)}}{\partial t} + \varepsilon \frac{\partial^2 E_\varphi^{(1)}}{\partial t^2} = F_p, \tag{1.5}$$

where the following notation is used:

$$F_q = \gamma + \frac{2\,\partial^2 D_{*\varphi}}{\partial E_\varphi^{(1)}\,\partial T}\frac{\partial T}{\partial t} + \frac{\partial^2 D_{*\varphi}}{\partial E_\varphi^{(1)2}}\frac{\partial E_\varphi^{(1)}}{\partial t};$$

$$F_p = -\frac{\partial^2 D_{*\varphi}}{\partial T^2}\Big(\frac{\partial T}{\partial t}\Big)^2 - \frac{\partial D_{*\varphi}}{\partial T}\frac{\partial^2 T}{\partial t^2} + \frac{\partial}{\partial r}\Big(\frac{1}{\mu_z}\frac{\partial B_{*z}}{\partial T}\frac{\partial T}{\partial t}\Big) - \frac{\partial}{\partial z}\Big(\frac{1}{\mu_r}\frac{\partial B_{*r}}{\partial T}\frac{\partial T}{\partial t}\Big).$$

In the following, we restrict ourselves to the case of an isotropic body: $\mu_r = \mu_z = \mu$.

We note that for quasisteady-state external electromagnetic effects, the effect of bias currents in the region of the electrically conducting body can be ignored compared to conduction currents [6]. In this case, Eq. (1.5) becomes parabolic (the term with the second time derivative vanishes); $F_p = \dfrac{\partial}{\partial r}\Big(\dfrac{1}{\mu}\dfrac{\partial B_{*z}}{\partial T}\dfrac{\partial T}{\partial t}\Big) - \dfrac{\partial}{\partial z}\Big(\dfrac{1}{\mu}\dfrac{\partial B_{*r}}{\partial T}\dfrac{\partial T}{\partial t}\Big)$ and $F_q = \gamma$.

The corresponding equation for the ambient medium is written as

$$-\frac{1}{\mu_0}\Big(\frac{\partial}{\partial r}\Big(\frac{1}{r}\frac{\partial}{\partial r}(rE_\varphi^{(0)})\Big) - \frac{\partial}{\partial z}\Big(\frac{\partial E_\varphi^{(0)}}{\partial z}\Big)\Big) + \varepsilon_0 \frac{\partial^2 E_\varphi^{(0)}}{\partial t^2} = -\frac{\partial j_\varphi^{(0)}}{\partial t}. \tag{1.6}$$

For the known electric strength $\boldsymbol{E}$ in the body–ambient-medium system, the magnetic induction is determined from the relation

$$B_r^{(m)} = \int\limits_0^t \frac{\partial E_\varphi^{(m)}}{\partial z}\, dt', \qquad B_z^{(m)} = -\int\limits_0^t \frac{1}{r}\,\frac{\partial (r E_\varphi^{(m)})}{\partial r}\, dt'. \tag{1.7}$$

The constraints on the EMF characteristics at the interface between the body S and the ambient medium are usually specified based on the Maxwell equations in integral form. In the absence of surface currents, these equations yield two independent conditions that define the equality of the tangential components of the electric and magnetic strength vectors [7]. For the case considered, these conditions are written in the functions $\boldsymbol{E}$ as follows:

$$E_\varphi^{(1)} = E_\varphi^{(0)}; \tag{1.8}$$

$$\Big(\mu^{-1}\,\frac{1}{r}\,\frac{\partial\,(r E_\varphi^{(1)})}{\partial r} - \mu_0^{-1}\,\frac{1}{r}\,\frac{\partial\,(r E_\varphi^{(0)})}{\partial r}\Big) n_r + \Big(\mu^{-1}\,\frac{\partial E_\varphi^{(1)}}{\partial z} - \mu_0^{-1}\,\frac{\partial E_\varphi^{(0)}}{\partial z}\Big) n_z = 0, \tag{1.9}$$

where $\boldsymbol{n} = (n_r, n_z)$ is the outward normal vector to the surface S.

We assume that the body is under conditions of convective heat transfer through the surface S with the ambient medium, whose temperature is T_S:

$$\lambda \boldsymbol{n} \cdot \nabla T + \beta (T - T_S) = 0. \tag{1.10}$$

Here $\beta = \beta(T)$ is the heat-transfer coefficient.

The conditions at infinity and on the Oz axis are written as

$$\frac{1}{r}\,\frac{\partial\,(r E_\varphi^{(0)})}{\partial r}\, n_r + \frac{\partial E_\varphi^{(0)}}{\partial z}\, n_z = 0; \tag{1.11}$$

$$E_\varphi = 0. \tag{1.12}$$

At the initial time, there is no EMF in the body and the ambient medium and the initial temperature distribution $T_0(r, z)$ is specified in the body.

The problem of determining the EMF in the body–ambient-medium system and the temperature distribution in the body reduces to solving Eqs. (1.3) and (1.5) for the body and Eq. (1.6) for the ambient medium subject to zero initial conditions on the electric strength, the specified initial temperature distribution $T_0(r, z)$, conditions (1.8)–(1.10) at the interface between the body the and ambient medium, conditions (1.11) at infinity and (1.12) on the Oz axis. The magnetic-induction components $\boldsymbol{B}$ are obtained from relation (1.7), the electric induction $\boldsymbol{D}$, and the magnetic strength $\boldsymbol{H}$, the differential dielectric permeability ε, and the magnetic permeability μ in the body are determined using the phenomenological relations (1.1).

If in determining the EMF, we use magnetic strength $\boldsymbol{H}$ as the computational function, then instead of one Eq. (1.5) we obtain two equations [for the unknowns $H_r(r, z, t)$ and $H_z(r, z, t)$], which should be solved simultaneously with Eq. (1.3). However, for a long electrically conducting cylindrical body under steady-state external electromagnetic action independent of the z coordinate, one nonzero component H_z is retained, for which, ignoring bias currents in the body, we obtain the equation

$$\frac{1}{r}\,\frac{\partial}{\partial r}\Big(r\,\frac{1}{\gamma}\,\frac{\partial H_z^{(1)}}{\partial r}\Big) - \mu\,\frac{\partial H_z^{(1)}}{\partial t} = \frac{\partial B_{*z}}{\partial T}\,\frac{\partial T}{\partial t}. \tag{1.13}$$

For the specified $H_z^{(1)}$ on the surface, the problem of determining the EMF and temperature in this case reduces to solving Eqs. (1.13) and the equation

$$c\,\frac{\partial T}{\partial t} = \frac{1}{r}\,\frac{\partial}{\partial r}\Big(\lambda r\,\frac{\partial T}{\partial r}\Big) + j_\varphi^{(1)} E_\varphi^{(1)} \qquad \Big(E_\varphi^{(1)} = \frac{1}{\gamma}\,\frac{\partial H_z^{(1)}}{\partial r}\Big) \tag{1.14}$$

with zero initial conditions on the magnetic strength, the specified initial temperature distribution $T_0(r, z)$, conditions of convective heat transfer on the cylinder surface (for $r = R$), and the conditions

$$\frac{\partial T}{\partial r} = 0, \qquad \frac{\partial H_z^{(1)}}{\partial r} = 0 \quad \text{at} \quad r = 0. \tag{1.15}$$

In the proposed computational model with the assumptions made above, the dynamic effect of the EMF on the electrically conducting body reduces to the action of ponderomotive forces [6], which vanish except for the Ampère force $\boldsymbol{F}^A$ and the force $\boldsymbol{F}^M$ exerted by the field on molecular currents, whose components are given by the relations

$$F_r^A = \gamma E_\varphi^{(1)} B_z^{(1)}, \qquad F_z^A = -\gamma E_\varphi^{(1)} B_r^{(1)},$$

$$F_r^M = \Big(\frac{1}{\mu_0} B_r^{(1)} - H_r^{(1)}\Big)\frac{\partial B_r^{(1)}}{\partial r} + \Big(\frac{1}{\mu_0} B_z^{(1)} - H_z^{(1)}\Big)\frac{\partial B_z^{(1)}}{\partial r},$$

$$F_z^M = \Big(\frac{1}{\mu_0} B_z^{(1)} - H_z^{(1)}\Big)\frac{\partial B_z^{(1)}}{\partial z} + \Big(\frac{1}{\mu_0} B_r^{(1)} - H_r^{(1)}\Big)\frac{\partial B_r^{(1)}}{\partial z}.$$

The temperature field and the ponderomotive forces obtained from the solution of the coupled problem of electrodynamics and heat conduction $\boldsymbol{F} = \boldsymbol{F}^A + \boldsymbol{F}^B$ are the basic parameters for determining the stress state of the body.

The stress–strain state of the body is analyzed using the relations for nonisothermal elastoplastic flow [9], according to which the deformation process is considered by steps. Starting with the specified values at $t = 0$, the ponderomotive forces and the temperature distribution in the body change by corresponding increments in each loading step, so that by the end of the deformation process they take the final values. In each step, using the specified increments of these forces and the temperature, we determine the displacement, strain, and stress increments, which are added to those obtained in the previous steps. Thus, step by step, we obtain the history of variation in the thermomechanical state of the body.

Let us consider the next loading step. Plastic deformation starts when a point in the stress space reaches the yield surface

$$\Phi(\sigma_{ij} - o_{ij}) = K^2\Big(\int d\varepsilon_i^p, T\Big), \tag{1.16}$$

where σ_{ij} are the stress-tensor components, o_{ij} are the coordinates of the center of the yield surface, K^2 is a function that specifies the dimension of the yield surface as a function of the temperature and the accumulated plastic strain $\int d\varepsilon_i^p$, and $d\varepsilon_i^p = \sqrt{(2/3)\, d\varepsilon_{ij}^p\, d\varepsilon_{ij}^p}$ is the rate of increment in the plastic strain. As the criterion of transition to plasticity, we use the Mises condition, for which the yield function is

$$\Phi(\sigma_{ij} - o_{ij}) = \sqrt{(3/2) s_{ij} s_{ij}}, \qquad s_{ij} = \sigma_{ij} - o_{ij} - (1/3)\delta_{ij}(\sigma_{ij} - o_{ij}). \tag{1.17}$$

Here δ_{ij} is the Kronecker delta.

The stress increment for a loading step is written as

$$d\sigma_{ij} = G_{ijkl}^{t+dt}(d\varepsilon_{kl} - d\varepsilon_{kl}^T - d\varepsilon_{kl}^p) + dG_{ijkl}(\varepsilon_{kl} - \varepsilon_{kl}^T - \varepsilon_{kl}^p). \tag{1.18}$$

Here G_{ijkl}^{t+dt} and dG_{ijkl} are the components of the elastic modulus tensor at the time $t+dt$ (at the end of the loading step) and their increments (as functions of temperature) in the given step; ε_{kl}, ε_{kl}^T, and ε_{kl}^p are components of the total-, temperature-, and plastic-strain tensors, respectively, at the time t (at the beginning of the step).

The plastic strain increments are determined using the associated plastic flow law on the development of plastic strains normal to the yield surface:

$$d\varepsilon_{ij}^p = d\chi\, \frac{\partial \Phi}{\partial \sigma_{ij}}. \tag{1.19}$$

The temperature-strain increment is given by

$$d\varepsilon_{ij}^T = \delta_{ij}(\alpha^{t+dt}\, dT + (\alpha^{t+dt} - \alpha^t)(T - T_0)), \tag{1.20}$$

where α is the thermal-expansion coefficient.

With allowance for relations (1.16)–(1.20), the relations between the stress and strain increments become [9]

$$d\sigma_{ij} = \left(G^{t+dt}_{ijmn} - \frac{G^{t+dt}_{ijvw} \dfrac{\partial \Phi}{\partial \sigma_{vw}} \dfrac{\partial \Phi}{\partial \sigma_{kl}} G^{t+dt}_{klmn}}{\dfrac{2}{3} H^t \dfrac{\partial \Phi}{\partial \sigma_{pq}} \dfrac{\partial \Phi}{\partial \sigma_{pq}} + G^{t+dt}_{pqrs} \dfrac{\partial \Phi}{\partial \sigma_{pq}} \dfrac{\partial \Phi}{\partial \sigma_{rs}}} \right) (d\varepsilon_{mn} - d\varepsilon^T_{mn})$$

$$+ \left(dG_{ijmn} - \frac{G^{t+dt}_{ijvw} \dfrac{\partial \Phi}{\partial \sigma_{vw}} \dfrac{\partial \Phi}{\partial \sigma_{kl}} dG_{klmn}}{\dfrac{2}{3} H^t \dfrac{\partial \Phi}{\partial \sigma_{pq}} \dfrac{\partial \Phi}{\partial \sigma_{pq}} + G^{t+dt}_{pqrs} \dfrac{\partial \Phi}{\partial \sigma_{pq}} \dfrac{\partial \Phi}{\partial \sigma_{rs}}} \right) (\varepsilon_{mn} - \varepsilon^p_{mn} - \varepsilon^T_{mn})$$

$$+ \frac{\sqrt{\dfrac{2}{3} \dfrac{\partial \Phi}{\partial \sigma_{kl}} \dfrac{\partial \Phi}{\partial \sigma_{kl}}}\, G^{t+dt}_{ijmn} \dfrac{\partial \Phi}{\partial \sigma_{mn}} \dfrac{\partial \sigma_i}{\partial T}}{\dfrac{2}{3} H^t \dfrac{\partial \Phi}{\partial \sigma_{pq}} \dfrac{\partial \Phi}{\partial \sigma_{pq}} + G^{t+dt}_{pqrs} \dfrac{\partial \Phi}{\partial \sigma_{pq}} \dfrac{\partial \Phi}{\partial \sigma_{rs}}} dT$$

or, in matrix-vector form,

$$\{d\sigma\} = [\boldsymbol{G}]^{t+\Delta t}(\{d\varepsilon\} - \{d\varepsilon_T\}) + [d\boldsymbol{G}](\{\varepsilon\}^t - \{\varepsilon_T\}^t - \{\varepsilon_p\}^t) + \{Z\}\, dT. \tag{1.21}$$

Here H^t is the slope of the curve of equivalent stresses σ_i versus equivalent plastic strains ε^p_i; $\{\varepsilon\} = \{\varepsilon_{rr}, \varepsilon_{\varphi\varphi}, \varepsilon_{zz}, 2\varepsilon_{rz}\}'$, $\{\sigma\} = \{\sigma_{rr}, \sigma_{\varphi\varphi}, \sigma_{zz}, \sigma_{rz}\}'$ (the prime denotes the transposition operation). We note that the appearance of the last two terms in Eq. (1.21) is due to the temperature dependence of the elastic properties and yield strength of the material.

We close the above system of equations by geometrical relations, restricting ourselves to the case of small strains, and the equilibrium equations [10]

$$\{\varepsilon\} = [\boldsymbol{A}]\boldsymbol{u}; \tag{1.22}$$

$$[\boldsymbol{A}]' \cdot \{\sigma\} - \boldsymbol{F} = 0 \tag{1.23}$$

with the known boundary conditions in displacement and stresses

$$([\Sigma_n]\{\sigma\} - \boldsymbol{p})\Big|_{S_\sigma} = 0, \qquad \boldsymbol{u}\Big|_{S_u} = \boldsymbol{u}^{(0)}, \qquad S_u \cup S_\sigma = S, \qquad S_u \cap S_\sigma = \varnothing. \tag{1.24}$$

Here $\boldsymbol{p}$ and $\boldsymbol{u}^{(0)}$ are the external loading vectors specified on the surface S_σ and the displacement vectors $\boldsymbol{u} = (u_r, u_z)$ specified on the surface S_u;

$$[\boldsymbol{A}] = \begin{bmatrix} \partial/\partial r & 1/r & 0 & \partial/\partial z \\ 0 & 0 & \partial/\partial z & \partial/\partial r \end{bmatrix}', \qquad [\Sigma_n] = \begin{bmatrix} n_r & 0 & n_z & 0 \\ 0 & n_z & n_r & 0 \end{bmatrix}'$$

are the matrices of the differential operator of the geometrical relations of elastic theory and the direction cosines of the normal to the surface S [10].

Thus, according to the proposed computational scheme, the problem of determining the stress–strain state of an electrically conducting solid body exposed to an external EMF is solved in two steps and consists of solving the coupled problem of electrodynamics, heat conduction, and thermal elasticity. In the second step, the displacement, strain, and stress are determined from the equilibrium equations (1.23), geometrical relations (1.22), and the equations of state (1.21) with boundary conditions (1.24) using the values of the temperature and ponderomotive forces obtained in the first step.

2. Solution Procedure. The formulated problem is solved using the finite-element method in the version of the method of weighted residuals [10]. Let us write the constitutive relations of the method for the coupled problem of electrodynamics and heat conduction. For this, we multiply the heat-conduction equation (1.3) by an arbitrary weight function $w \in H^1(V)$ [Sobolev's space $H^1(V) = \{w \in L^2(V),\ \nabla w \in L^2(V)\}$] and integrate the obtained relation over the domain V. Using the Green formula and the heat-transfer condition (1.10), we obtain

$$\int\limits_V \Big(c \frac{\partial T}{\partial t} w + \lambda \Big(\frac{\partial T}{\partial r} \frac{\partial w}{\partial r} + \frac{\partial T}{\partial z} \frac{\partial w}{\partial z} \Big) - j^{(1)}_\varphi E^{(1)}_\varphi w \Big) r\, dr\, dz + \int\limits_S \beta (T - T_c) w r\, d\xi = 0. \tag{2.1}$$

We apply the same approach to Eqs. (1.5) and (1.6), previously replacing the infinite space in it by a finite domain V_* ($V \subset V_*$) bounded by a surface S_* remote from the body and the currents considered. Using the Green formula we obtain the relations

$$\int\limits_V \mu^{-1}\Big(\frac{1}{r}\,\frac{\partial\,(rE_\varphi^{(1)})}{\partial r}\,\frac{1}{r}\,\frac{\partial\,(rw_1)}{\partial r}+\frac{\partial E_\varphi^{(1)}}{\partial z}\,\frac{\partial w_1}{\partial z}\Big)r\,dr\,dz$$

$$+\int\limits_S \mu^{-1}\Big(\frac{1}{r}\,\frac{\partial\,(rE_\varphi^{(1)})}{\partial r}\,n_r+\frac{\partial E_\varphi^{(1)}}{\partial z}\,n_z\Big)w_1 r\,d\xi$$

$$+\int\limits_V \Big(\frac{\partial\gamma}{\partial t}\,E_\varphi^{(1)}+F_q\,\frac{\partial E_\varphi^{(1)}}{\partial t}+\varepsilon\,\frac{\partial^2 E_\varphi^{(1)}}{\partial t^2}-F_p\Big)w_1 r\,dr\,dz=0\quad\forall\ w_1\in H^1(V_*);$$

$$\int\limits_{V_*\setminus V} \mu_0^{-1}\Big(\frac{1}{r}\,\frac{\partial\,(rE_\varphi^{(0)})}{\partial r}\,\frac{1}{r}\,\frac{\partial\,(rw_1)}{\partial r}+\frac{\partial E_\varphi^{(0)}}{\partial z}\,\frac{\partial w_1}{\partial z}\Big)r\,dr\,dz$$

$$+\int\limits_{V_*\setminus V}\varepsilon_0\,\frac{\partial^2 E_\varphi^{(0)}}{\partial t^2}w_1 r\,dr\,dz-\int\limits_S \mu_0^{-1}\Big(\frac{1}{r}\,\frac{\partial\,(rE_\varphi^{(0)})}{\partial r}n_r+\frac{\partial E_\varphi^{(0)}}{\partial z}\,n_z\Big)w_1 r\,d\xi$$

$$+\int\limits_{V_*\setminus V}\frac{\partial j_\varphi}{\partial t}\,w_1 r\,dr\,dz=0\qquad\forall\ w_1\in H^1(V_*). \tag{2.2}$$

Here $H^1(V_*)=\{w\in H^1(V_*)\colon\ w=0\ \forall\ (0,z)\in V_*\}$. Satisfying boundary conditions (1.12), the weight function on the Oz axis vanishes. The minus sign appears in relation (2.2) because $\boldsymbol{n}$ is an inward (with respect to the ambient medium $V_*\setminus V$) normal to the surface S. The integral over S_* vanishes by virtue of boundary conditions (1.11).

Using conditions (1.9), we arrive at the following unified relation for the problem of electrodynamics written for the entire domain V_*:

$$\int\limits_{V_*} \mu_c^{-1}\Big(\frac{1}{r}\,\frac{\partial\,(rE_\varphi)}{\partial r}\,\frac{1}{r}\,\frac{\partial\,(rw_1)}{\partial r}+\frac{\partial E_\varphi}{\partial z}\,\frac{\partial w_1}{\partial z}\Big)r\,dr\,dz$$

$$+\int\limits_{V_*}\Big(\gamma_t E_\varphi+F_c\,\frac{\partial E_\varphi}{\partial t}+\varepsilon_c\,\frac{\partial^2 E_\varphi}{\partial t^2}+F_d\Big)w_1 r\,dr\,dz=0\qquad\forall\ w_1\in H^1(V_*). \tag{2.3}$$

Here the following notation is introduced: for the region of the body V,

$$\mu_c=\mu;\quad \varepsilon_c=\varepsilon;\quad \gamma_t=\frac{\partial\gamma}{\partial t};\quad F_c=F_q;\quad F_d=-F_p;\quad E_\varphi=E_\varphi^{(1)};$$

for the ambient medium $V_*\setminus V$,

$$\mu_c=\mu_0;\quad \varepsilon_c=\varepsilon_0;\quad \gamma_t=0;\quad F_c=0;\quad F_d=\frac{\partial j_\varphi}{\partial t};\quad E_\varphi=E_\varphi^{(0)}.$$

Let us perform the standard procedure of finite-element discretization of relations (2.1) and (2.3) over the spatial variables [10]. In this case, the domain V_* is partitioned in such a manner that the interface between the body and the ambient medium coincides with the boundaries of the corresponding finite elements. As a result, we obtain the system of ordinary differential equations

$$[L_1]\{\dot T_h(t)\}+[L_0]\{T_h(t)\}=\{f_T\},\qquad \{T_h(0)\}=\{T_h^0\}; \tag{2.4}$$

$$[M_2]\{\ddot E_h(t)\}+[M_1]\{\dot E_h(t)\}+[M_0]\{E_h(t)\}=\{f_E\},\quad \{E_h(0)\}=0,\quad \{\dot E_h(0)\}=0 \tag{2.5}$$

for the unknown temperature $\{T_h\}$ and electric strength $\{E_h\}$ at the partition nodes. The matrix-vector characteristics of the obtained system of equations are calculated by summing the corresponding characteristics of individual finite elements:

$$[L_0]^{el} = \int\limits_{V^{el}} \lambda\Big(\Big[\frac{\partial N}{\partial r}\Big]'\Big[\frac{\partial N}{\partial r}\Big] + \Big[\frac{\partial N}{\partial z}\Big]'\Big[\frac{\partial N}{\partial r}\Big]\Big) r\,dr\,dz + \int\limits_{S^{el}} \beta[N]'[N] r\,d\xi,$$

$$[L_1]^{el} = \int\limits_{V^{el}} c[N]'[N] r\,dr\,dz, \qquad \{f_T\}^{el} = \int\limits_{V^{el}} j_\varphi^{(1)} E_\varphi^{(1)}[N]' r\,dr\,dz + \int\limits_{S^{el}} \beta[N]' r\,d\xi,$$

$$[M_0]^{el} = \int\limits_{V_*^{el}} \frac{1}{\mu_c}\Big(\Big[\frac{\partial N}{\partial r}\Big]'\Big[\frac{\partial N}{\partial r}\Big] + \Big[\frac{\partial N}{\partial z}\Big]'\Big[\frac{\partial N}{\partial z}\Big]\Big) r\,dr\,dz + \int\limits_{V_*^{el}} \gamma_t[N]'[N] r\,dr\,dz$$

$$+ \int\limits_{V_*^{el}} \frac{1}{\mu_c}\frac{1}{r}\Big(\Big[\frac{\partial N}{\partial r}\Big]'[N] + [N]'\Big[\frac{\partial N}{\partial r}\Big] + \frac{1}{r}[N]'[N]\Big) r\,dr\,dz,$$

$$[M_1]^{el} = \int\limits_{V_*^{el}} F_c[N]'[N] r\,dr\,dz, \qquad [M_2]^{el} = \int\limits_{V_*^{el}} \varepsilon_c[N]'[N] r\,dr\,dz, \qquad \{f_E\}^{el} = \int\limits_{V_*^{el}} F_d[N]' r\,dr\,dz.$$

Here $[N] = [N_1, N_2, \ldots, N_l]$, $[\partial N/\partial r]$, $[\partial N/\partial z]$ are the matrices of the shape functions and their derivatives and l is the number of finite-element nodes.

The Cauchy problem (2.4), (2.5) is solved using the family of simple one-step multiparameter algorithms known as the Zienkiewicz–Wood method [11]. In this case, the temperature dependences of the electrophysical and thermal characteristics and the dependences of the electric and magnetic inductions on the corresponding strengths are approximated by interpolation splines constructed on the basis of real curves that describe the solid body behavior in EMF.

For the case of a long cylinder, problem (1.13)–(1.15) is solved similarly.

Using the known parameters describing the EMF in the body, we calculate the ponderomotive forces and pass to the second step of the solution of the problem.

Let us write the basic finite-element relations for the thermoelastic problem. With allowance for the equilibrium of the stress state at the beginning of the loading step, the incremental stress equilibrium equation for the body becomes [10]

$$[\boldsymbol{A}]'\{d\sigma\} - \{d\boldsymbol{F}\} = 0. \tag{2.6}$$

Substituting the physical relations (1.21) and geometrical relations (1.22) into (2.6), using the standard procedure of the method of weighted residuals, and introducing finite-element approximations, we obtain the incremental displacement equilibrium equation [10]

$$[\boldsymbol{K}_{ep}]\{d\boldsymbol{q}\} = \{d\boldsymbol{F}\} + \{d\boldsymbol{P}\} + \{d\boldsymbol{R}\},$$

which is solved using the method of variable rigidity parameters [10]. Here $\{d\boldsymbol{q}\}$ is the global vector of nodal-displacement increments; the matrix-vector characteristics $[\boldsymbol{K}_{ep}]$, $\{d\boldsymbol{F}\}$, and $\{d\boldsymbol{P}\}$ are obtained by summing up the corresponding characteristics of individual elements:

$$[\boldsymbol{K}_{ep}^{(el)}] = \int\limits_{V^{el}} [\boldsymbol{N}]'[\boldsymbol{A}]'[\boldsymbol{C}]^{t_j+\Delta t_j}[\boldsymbol{A}][\boldsymbol{N}] r\,dr\,dz,$$

$$\{d\boldsymbol{P}\}^{(el)} = \int\limits_{V^{el}} [\boldsymbol{N}]'[\boldsymbol{A}]'([d\boldsymbol{C}](\{\varepsilon\} - \{\varepsilon_T\} - \{\varepsilon_p\}) + \{z\}\,dT) r\,dr\,dz + \int\limits_{S_\sigma^{(el)}} [\boldsymbol{N}]'\{d\boldsymbol{p}\} r\,d\xi,$$

$$\{d\boldsymbol{R}^{(el)}\} = \int\limits_{V^{el}} [\boldsymbol{N}]'[\boldsymbol{A}]'[\boldsymbol{A}][\boldsymbol{N}]\{d\varepsilon_T\} r\,dr\,dz, \qquad \{d\boldsymbol{F}^{(el)}\} = \int\limits_{V^{el}} [\boldsymbol{N}]'\{d\boldsymbol{F}\} r\,dr\,dz.$$

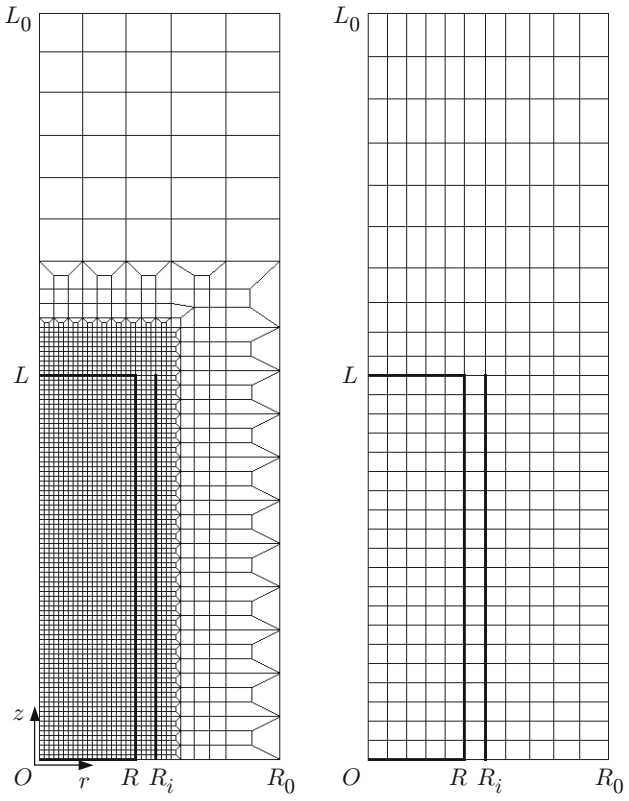

Fig. 1

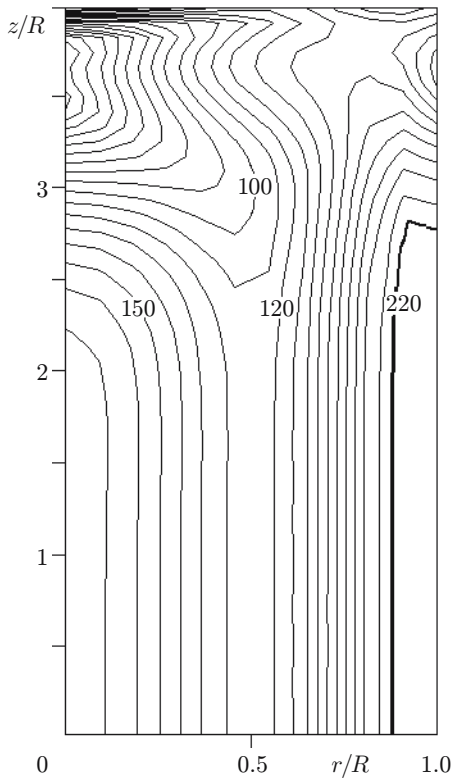

Fig. 2

Fig. 1. Standard finite-element meshes.

Fig. 2. Stress intensity in a cylinder of Kh18N9T steel ($t = 7.1$ sec): the numbers at the lines refer to σ (σ in MPa).

The proposed technique was used to design the corresponding software for modeling the interaction of electromagnetic, temperature, and mechanical fields in an electrically conducting body exposed to an external EMF and to solve a number of particular problems.

3. Induction Heating of a Cylinder. As an example, we consider the induction heating a steel cylinder of length $2L$ and radius R free from dynamic loading. The cylinder is in an inductor which is coaxial with it and is modeled by a cylindrical surface of radius R_i and length $2L_i$. The current flowing in the inductor has density

$$\boldsymbol{j}^{(0)}(r, z, t) = (0, J_0 \sin(2\pi\omega t), 0), \qquad r = R_i, \qquad |z| \leqslant L_i, \tag{3.1}$$

where ω is the frequency.

To study the convergence of the numerical schemes, we solved the problem using finite-element meshes of various densities with various integration time steps, and various dimensions of the domain V_*. The results were compared with known analytical solutions.

Figure 1 shows the standard meshes of isoparametric biquadratic eight-nodal elements used in the calculations [10] ($R = 0.01$ m, $L = 0.04$ m, $R_i = 0.012$ m, $L_i = 0.042$ m, $R_0 = 2.5R$, and $L_0 = 2L$).

3.1. *Cylinder of Nonferromagnetic* Kh18N9T *Steel.* The characteristics of the steel are known [7] (their temperature dependence was ignored). The calculations were performed for $J_0 = 6 \cdot 10^4$ A/m^2, $\omega = 3 \cdot 10^5$ Hz, $\beta = 167$ W/(m$^2\cdot$K), and $T_0 = T_S = 0°$C. The elastic limit was set equal to 220 MPa.

Figure 2 shows the stress intensity σ_i in the cylinder at $t = 7.1$ sec (the inductor-switching time in [7]). The edge effect covers an area of dimension $2R$. In the central part of the cylinder, the solution hardly depends on the z coordinate. The stresses σ_{rr}, σ_{zz}, and $\sigma_{\varphi\varphi}$ in the equatorial section of the cylinder $z = 0$ are given in Fig. 3. For comparison, the dashed lines in the same figure show known analytical solutions obtained in closed form for

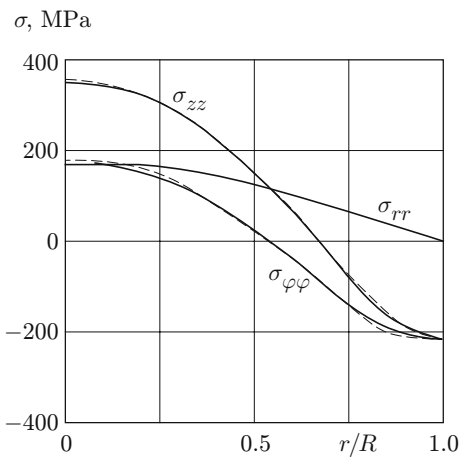

Fig. 3

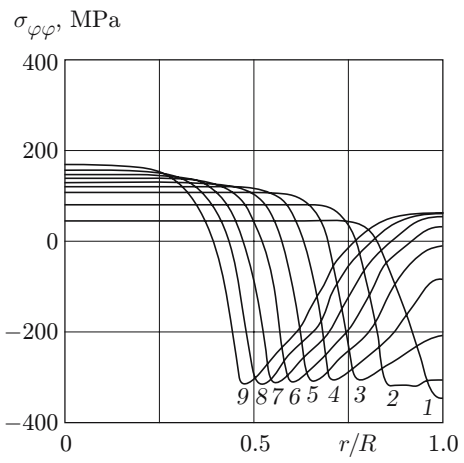

Fig. 4

Fig. 3. Stresses in the cross section $z = 0$ of the cylinder ($t = 7.1$ sec).

Fig. 4. Stresses $\sigma_{\varphi\varphi}$ in the cylinder of S30 steel under heating: $t =$ 0.007 (1), 0.02 (2), 0.04 (3), 0.06 (4), 0.08 (5), 0.10 (6), 0.12 (7), 0.14 (8), and 0.159 sec (9).

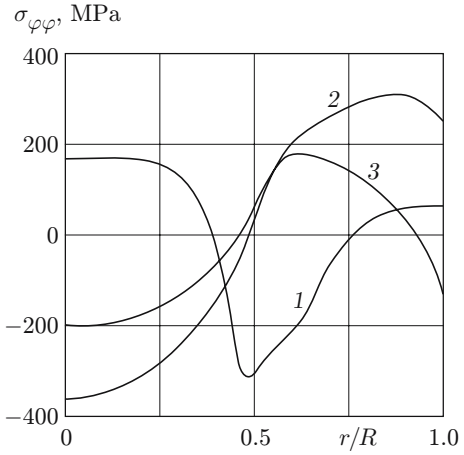

Fig. 5

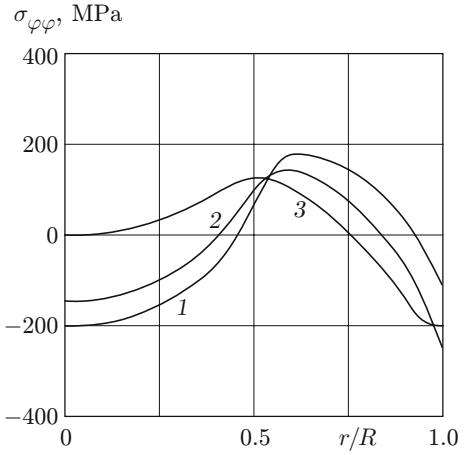

Fig. 6

Fig. 5. Stresses $\sigma_{\varphi\varphi}$ in the cylinder of S30 steel under cooling: $t =$ 0.159 (1), 2.45 (2), and 20 sec (3).

Fig. 6. Residual stresses $\sigma_{\varphi\varphi}$ in a cylinder of S30 steel.

a long cylinder in [7]. In the scale of the figure, the solutions almost coincide. This agreement of the results is obtained even for five eight-nodal elements on the radius of the cylinder (see Fig. 1b) and an integration time step $\Delta t_E = \omega^{-1}/16$.

It should be noted that the replacement of the external space by a domain V_* with parameters $R_0 = 2.5R$ and $L_0 = 2L$ (Fig. 1) does not influence the solution of the problem of electrodynamics and heat conduction: for $R_0 > 2.5R$ and $L_0 > 2L$, the solutions coincide with each other, and in the section $z = 0$, they are nearly identical to the solution of the one-dimensional problem (1.13)–(1.15) for a long cylinder with the boundary condition $H_z = 6 \cdot 10^4 \sin(2\pi\omega t)$ A/m specified on the cylinder surface (for $R_0 < 2.5R$ and $L_0 < 2L$, these solutions differ).

Because an analysis of the three fields of various natures with the same time step is ineffective from the point of view of computing costs, the algorithm for solving the problem provides for the use of different integration time

steps for the equations of electrodynamics, heat conduction, and elastoplasticity. In this case, the heat-conduction and elastoplastic equations contain the heat releases and ponderomotive forces averaged over the electromagnetic-wave oscillation period [12]. Thus, the solution of the problem obtained for an integration time step for the heat conduction equation $\Delta t_T = 2.367$ sec and a load step $\Delta t_M = 7.1$ sec almost coincides with the solution for $\Delta t_M = \Delta t_T = \Delta t_E$.

3.2. *Cylinder of Ferromagnetic* S30 *Steel*. The electrical, thermal, and physicomechanical characteristics of the steel and their temperature dependences are given in [5, 12–15]. The cylinder was heated by a current (3.1) ($J_0 = 10^6$ A/m^2 and $\omega = 8 \cdot 10^3$ Hz). Once the outer layer of the cylinder 1.5 mm thick was heated to a temperature $T \geqslant 970$°C, the current was switched off and the cylinder was cooled by convective heat transfer [$\beta = 10^4$ W/(m$^2\cdot$ K)] with the ambient medium, whose temperature was $T_S = 20$°C [for heating, $\beta = 13$ W/(m$^2\cdot$ K)]; $T_0 = T_S$.

An analysis of the results shows that when the outer layers of the cylinder are heated to the Curie temperature (770°C) and lose ferromagnetic properties, the maximum specific powers of the sources are shifted to the depth of the cylinder and the main heat release occurs in the region where the material has not yet lost ferromagnetic properties. In this case, the magnetic-field penetration depth increases during heating of the cylinder.

At the beginning of the heating process, compressing stresses arise in the surface layer and rapidly reach the elastic limit (curve 1 in Fig. 4). When this layer loses ferromagnetic properties, the region of the main heat release and maximum compressing stress is shifted to the interior of the cylinder (curves 2–9 in Fig. 4). As we can see, this leads to unloading of the surface layer.

When the required heating depths is reached, the current is switched off ($t = 0.159$ sec). Rapid cooling of the surface layer begins. In this layer, tensile stresses arise and rapidly increase, reaching the maximum at the time $t = 2.45$ sec (curve 2 in Fig. 5). The inner layers are cooled more slowly. Reducing in size under cooling, they contract the rapidly cooled surface layer and weaken the tensile stresses in it, whose maximum is shifted from the surface to the interior of the cylinder. As a result, residual compressing stresses occur in the surface layer (curve 3 in Fig. 5).

Figure 6 shows the residual stresses $\sigma_{\varphi\varphi}$ in the cylinder are shown (curve 1). For comparison, the same figure gives the residual stresses obtained ignoring the ferromagnetic properties of the material (with the magnetic permeability averaged over the magnetic density; curve 2) and with the constant physicomechanical characteristics averaged over the heating–cooling temperature range (curve 3).

Even at 300°C, the temperature distributions obtained taking into account the temperature dependence of the electrophysical characteristics begin to differ from the distributions calculated for the characteristics averaged over the heating time. During further heating, the difference begins even more considerable and gains a qualitative nature.

In this case, the effect of ponderomotive forces can be ignored. The maximum values of the dynamic stresses due to body forces are not less than 1% of the maximum temperature stresses.

A numerical convergence study shows that allowance for the ferromagnetic properties and temperature dependence of the material properties places far more stringent requirements on the discrete model. Thus, to obtain fairly exact values of the magnetic-field strength, one needs 500 elements along the radius of the cylinder for time steps $\Delta t_E = \omega^{-1}/2500$ and $\Delta t_T = \omega^{-1}$. To solve the elastoplastic problem, twenty finite elements along the radius of the cylinder are sufficient. The load step was variable. As soon as the maximum rise in the temperature at any point of the cylinder exceeded 15°C, the displacement, strain, and stress increments for the specified loading step were determined.

Conclusions. The above procedure for modeling thermomechanical processes in electrically conducting solids exposed to an external EMF provides a more adequate prediction of the behavior of articles made of magnetic materials over a wide range of temperatures. This is required for the automation of induction treatment, in particular, to estimate residual stresses, which are the initial stresses in the development of operation modes.

In modeling the processes of high-temperature induction heating of articles made of ferromagnetic steels, one needs to allow for the temperature dependence of the electric, thermal, and mechanical characteristics of the material. Otherwise, one obtains qualitatively different distributions of process parameters.

REFERENCES

1. C. Chaboudez, S. Clain, R. Glardon, et al., "Numerical modeling in induction heating for axisymmetric geometries," *IEEE Trans. Magn.*, **33**, No. 1, 735–745 (1997).
2. Y. Favennec, V. Labbe, and F. Bay, "Induction heating processes optimization a general optimal control approach," *J. Comput. Phys.*, **187**, 68–94 (2003).
3. V. Nemkov and R. Goldstein, "Calculater simulation for fundamental study and practical solutions to induction heating problems," *Int. J. Comput. Math. Electr. Electron. Eng.* (COMPEL), **22**, No. 1, 181–191 (2003).
4. J. Rappaz and M. Swierkosz, "Mathematical modeling and simulation of induction heating processes," *Appl. Math. Comp. Sci.*, **6**, No. 2, 207–221 (1996).
5. J. Turowski, *Elektrodynamika Techniczna*, WNT, Warszawa (1993).
6. A. Gaczkiewicz and Z. Kasperski, "Modele i metody matematyczne w zagadnieniach brzegowych termomechaniki cial przewodzacych," OW. Politechnika Opolska, Opole (1999).
7. Ya. S. Podstrigach, Ya. I. Burak, A. R. Gachkevich, and L. V. Chernyavskaya, *Thermoelasticity of Electrically Conducting Solids* [in Russian], Naukiva Dumka, Kiev (1977).
8. G. F. Golovin amd M. M. Zamyatin, *High-Frequency Thermal Treatment* [in Russian], Mashinostroenie, Leningrad (1990).
9. D. H. Allen and W. E. Heisler, "A theory for analysis of thermoplastic materials," *Comput. Struct.*, **13**, 129–135 (1981).
10. O. C. Zienkiewicz and R. L. Taylor, *Finite Element Method,* Vol. 1: *The Basis*, Butterworth Heinemann, London (2000).
11. O. C. Zienkiewicz, W. L. Wood, and N. W. Nine, "A unified set of single step algorithm," *Int. J. Numer. Methods Eng.*, **20**, 1529–1552 (1984).
12. T. Skoczkowski and M. Kalus, "The mathematical model of induction heating of ferromagnetic pipes," *IEEE Trans. Magn.*, No. 3, 2745–2750 (1989).
13. E. R. Khismatulin, E. M. Korolev, V. I. Livshits, et al., *High-Pressure Containers and Pipelines: Handbook* [in Russian], Mashinostroenie, Moscow (1990).
14. A. A. Preobrazhenskii, *Magnetic Materials and Units* [in Russian], Vysshaya Shkola, Moscow (1976).
15. I. K. Kikoin (ed.), *Table of Physical Quantities: Handbook* [in Russian], Atomizdat, Moscow (1976).